

Adapting Solar Cells With Polysilicon Passivated Contacts to Radiation-Rich Environments

Nicolas Enjalbert¹ , Romain Cariou¹ , and Sébastien Dubois¹ 

¹ Univ. Grenoble Alpes, CEA, Liten, Campus Ines, 73375 Le Bourget du Lac, France

*Correspondence: Nicolas Enjalbert, nicolas.enjalbert@cea.fr

Abstract. In the context of increased space photovoltaic power needs and cost reduction pressures, silicon solar cells spark a new interest for space missions. This is even truer if the cost-effective mass-produced silicon technologies can be adapted to the specific constraints of the space environment. This study successfully demonstrated that cells with polycrystalline silicon-based passivated contacts could be adapted to the main prerequisites for space missions. Indeed, flexible and lightweight alternative polysilicon passivated contacts cells were prepared from gallium-doped substrates, with post-irradiation performances as good as those of conventional (thicker) PERC devices. The influence of the doping level was investigated. Low doping levels mitigate the radiation-induced degradation of the bulk carrier lifetime and therefore of the short-circuit current density, but result in lower open circuit voltages. Furthermore, it was shown that the surface and bulk hydrogenation step investigated in this study does not influence the post-irradiation effective carrier lifetime and its evolution under prolonged illumination in the temperature range 80°C-100°C (at least for the durations investigated here).

Keywords: TOPCon, Space Irradiation, Hydrogen

1. Introduction

Nowadays, space solar cells essentially consist in expensive III-V multi-junction devices with high performances but limited production capacities. In the context of increased space photovoltaic (PV) power needs and cost reduction pressures, silicon (Si) solar cells spark a new interest. This is even truer if the cost-effective mass-produced Si technologies can be adapted to the specific constraints of the space environment. The two main Si devices that are replacing the standard Passivated Emitter and Rear Contact (PERC) cell for terrestrial uses are the amorphous Si (a-Si) / crystalline Si (c-Si) HeteroJunction (SHJ) cell and the so-called TOPCon cell. TOPCon refers to Tunnel Oxide Passivated Contact. Industrial TOPCon cells feature a polycrystalline Si (Poly-Si) on Si oxide (SiO_x) passivated contact on the rear side of the device and a boron-diffused emitter on the front side. Both technologies (i.e., SHJ and TOPCon) usually rely on the use of n-type Si wafers.

In space, Si solar cells suffer from electrons and protons irradiation-induced damages, causing severe bulk carrier lifetime (τ_b) degradations. There are usually three main levers for limiting the related efficiency (η) losses: i) p-type substrates (which feature a better radiation hardness than n-type Si) ii) front emitter architectures and iii) thin wafers [1], [2]. The last two levers significantly improve the carrier collection with low minority carrier diffusion length (L_{min}) materials. It is worth noting that beyond improving the radiation hardness, thin wafers offer interesting benefits such as lightweight solar generators and flexible PV arrays.

One may wonder about the relevance of having passivated contacts cells for environments inducing strong τ_b decreases. However, several recent studies showed that the radiation-induced defects could be *cured* (i.e., annihilation or passivation) by low-temperature annealing steps under illumination, representative of the real operating conditions (e.g., [3]). After such healing steps, the open-circuit-voltage (V_{oc}) of irradiated SHJ cells could exceed 720 mV [3], demonstrating the importance of having cells with advanced surface passivation. The underlying mechanisms are still matter of debates. They might be favoured by impurities such as hydrogen (H) [4].

Several research groups and companies recently communicated on SHJ cells for space (e.g., [3], [5]). The adaptation of SHJ cells to the main prerequisites for space missions is quite straightforward. Indeed, by using a p-type Si substrate, the cell features a front emitter. Furthermore, both the cell architecture (symmetric) and its fabrication process (low temperature, wafers relying on trays) are rather compliant with thin (i.e., $<90 \mu\text{m}$) wafers.

The adaptation of TOPCon cells for space raises more challenges. Indeed, with p-type wafers, the device features a rear emitter. Furthermore, the cell fabrication process is less adapted to very thin wafers (high temperature steps, asymmetric structure). The goal of this study concerns the development of an alternative TOPCon cell, compliant with the main prerequisites for space missions.

2. Experimental approach

This alternative TOPCon relies on a cell architecture featuring double-side Poly-Si on SiO_x stacks [6]. Ultra-thin Poly-Si layers (thickness $\leq 15 \text{ nm}$) are used to limit the optical losses. n-type and p-type Poly-Si films are formed on the front (textured) and rear (polished) surfaces, respectively, leading to a front emitter device with p-type substrates. Both Poly-Si films are capped by Indium Tin Oxide (ITO) layers contacted with screen-printed Ag (low-temperature) pastes (Fig. 1-a). Two different fabrication processes are tested (Fig. 1-b). The first relies on the double-side Low Pressure Chemical Vapor Deposition (LPCVD) of intrinsic a-Si layers *ex situ* doped by plasma immersion ion implantation. The second consists in the Plasma-Enhanced Chemical Vapor Deposition (PECVD) of *in situ* doped a-Si layers. The a-Si deposition and doping steps are followed by a dopant activation annealing step (925°C). Interestingly, both approaches (i.e. LPCVD- and PECVD-based) rely on lean fabrication processes, *a priori* well adapted to thin wafers.

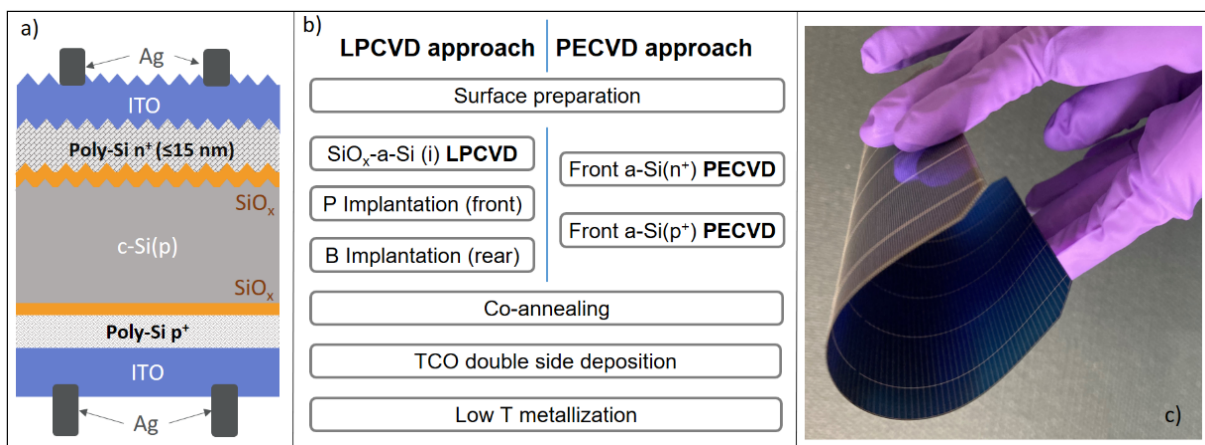


Figure 1. a) Schematic view of the adapted Poly-Si/SiO_x passivated contacts cells. b) Studied fabrication processes. c) Photograph of the 60 μm -thick solar cell.

One possible drawback of the developed cell could be related to the lack of H within the substrate since the process does not combine H-rich dielectric layers and firing steps. Even

if H-rich a-Si layers are deposited, H atoms exo-diffuse during the dopant activation annealing step [7]. As the influence of H on the passivation of radiation-induced defects is still a matter of debate, we prepared symmetric surface-passivated structures (with poly-Si(n⁺)/SiO_x stacks) for effective carrier lifetime (τ_{eff}) evaluations (Fig. 3, inset). The surfaces of the first structure feature ITO layers. Therefore, this structure did not experience any hydrogenation steps. The surfaces of the second structure were capped with H-rich dielectrics and the samples were fired. Thus, both the bulk and surfaces should contain H.

Notice that both the solar cells and symmetric precursors were prepared from Czochralski-grown gallium (Ga)-doped substrates. Two groups of adjacent wafers (referred to as Ga0.9 and Ga20) were used, with different resistivity (ρ) values (0.9 $\Omega\cdot\text{cm}$ and 20 $\Omega\cdot\text{cm}$, respectively) and interstitial oxygen concentrations ($7.7\times 10^{17}\text{ cm}^{-3}$ and $6.0\times 10^{17}\text{ cm}^{-3}$, respectively). Interestingly, such Ga-doped substrates would feature a better radiation hardness than boron (B)-doped wafers [8], even if the existing literature should be consolidated by further studies. The wafers were thinned by chemical etching, with two post-texturation thicknesses studied, 140 μm and 60 μm . The cells and lifetime samples were irradiated by electrons (1 MeV exposure, with doses ranging from 1.5×10^{14} to $1.5\times 10^{15}\text{ e/cm}^2$). Their properties (e.g., I-V, τ_{eff}) were assessed before and after irradiation.

3. Results and discussions

3.1. Solar cells processing

First, both processes allowed the elaboration of lightweight and flexible 60 μm -thick cells (Fig. 1-c). Issues were experienced with the back-end steps (ITO deposition & metallization) which limited the V_{oc} (i.e. maximum value of 686 mV with the LPCVD route whereas the post-annealing implied- V_{oc} ranged between 697 and 703 mV and are normally maintained during the subsequent steps). This limited the corresponding η values, with for the Ga20 60 μm -thick cells a maximum η of 19.2%. We did not observe any significant effects of both the ρ and substrate thickness on the initial η . Lower and more scattered performances were obtained with the PECVD route, but they may be due to the back-end issues previously mentioned (no specific problems identified on the post-annealing implied- V_{oc}). It is also worth noting that these V_{oc} are high enough to allow relevant investigations of the radiation effects (since they are known for inducing severe τ_{b} degradations).

3.2. Post-irradiation photovoltaic performances

Fig. 2 presents the variation of the short-circuit current density (J_{sc}), V_{oc} and η of the 60 μm -thick cells (processed via the LPCVD route), as a function of the electron irradiation fluence. The results are compared with those obtained for a standard 180 μm -thick PERC cell.

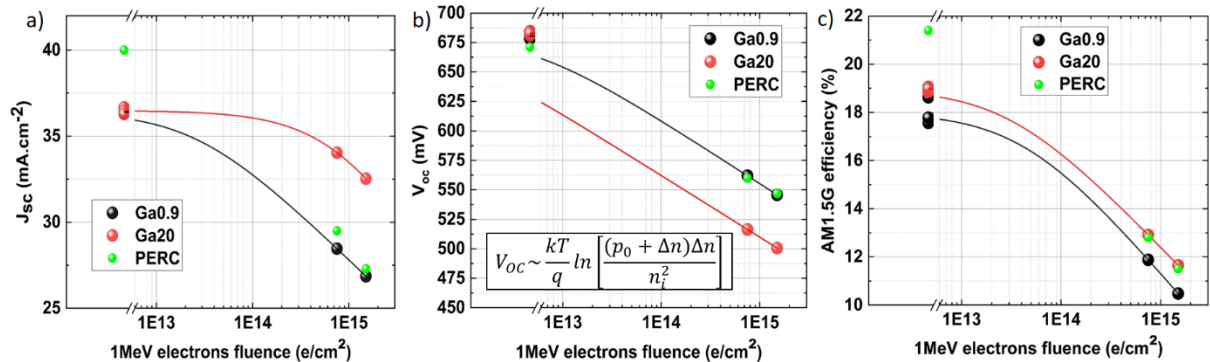


Figure 2. Variations of the J_{sc} , V_{oc} and η with the irradiation dose. Solid lines are only guides to the eye.

Focusing on the J_{sc} , interestingly, its decrease with the irradiation fluence was significantly stronger for the cells with the low ρ . To get further insights, the effective L_{min} were extracted from the spectral variation of the Internal Quantum Efficiency in the infrared range for 140 μm thick samples irradiated at a fluence of $1.5 \times 10^{14} \text{ cm}^{-2}$. The L_{min} were equal to 74 μm and 354 μm for the 0.9 $\Omega\cdot\text{cm}$ and 20 $\Omega\cdot\text{cm}$ ρ , respectively. This highlights a significant influence of the substrate doping level on the post-irradiation τ_b . This is in good agreement with the results from [4], which showed (for B-doped Si) that the τ_b -limiting radiation-induced defects (attributed to vacancies) would introduce shallow energy levels in the Si band gap, with a recombination strength enhanced by high equilibrium majority carrier concentrations (p_0). Notice that a J_{sc} higher than 32 $\text{mA}\cdot\text{cm}^{-2}$ for the 20 $\Omega\cdot\text{cm}$ solar cells at a fluence of $1.5 \times 10^{15} \text{ e}^-/\text{cm}^2$ might appear a bit surprising, since for these conditions the τ_{eff} is only around 0.6 μs . However, such a τ_{eff} corresponds to a L_{min} of about 46 μm , in the range of the cell's thickness, meaning that a large fraction of the photogenerated charge carriers can be collected. Furthermore, these results were well reproduced by simple PC1D simulations (not shown here). Regarding the V_{oc} , an opposite trend with the substrate ρ is observed, well explained by the equation in the inset of Fig. 2-b, since after irradiation, $\Delta n \ll p_0$ (Δn being the excess carrier density). About the η , for a given irradiation dose, eventually the best η are obtained with the 20 $\Omega\cdot\text{cm}$ ρ , demonstrating the importance of fine optimizations of this parameter. Furthermore, for such ρ , the post-irradiation η of the lightweight and flexible alternative TOPCon cell is as good as the values determined for standard 180 μm -thick PERC cells.

3.3 Influence of hydrogenation steps

Fig. 3 shows the post-irradiation τ_{eff} values (obtained by quasi-steady-state photoconductance decay) of symmetric precursors (20 $\Omega\cdot\text{cm}$ Ga-doped samples) without and with the hydrogenation step, for different irradiation fluences. First, these data confirm the strong decrease of τ_{eff} due to electrons irradiation, the higher the irradiation fluence, the lower the τ_{eff} . Furthermore, the results show that the implemented hydrogenation step does not influence τ_{eff} .

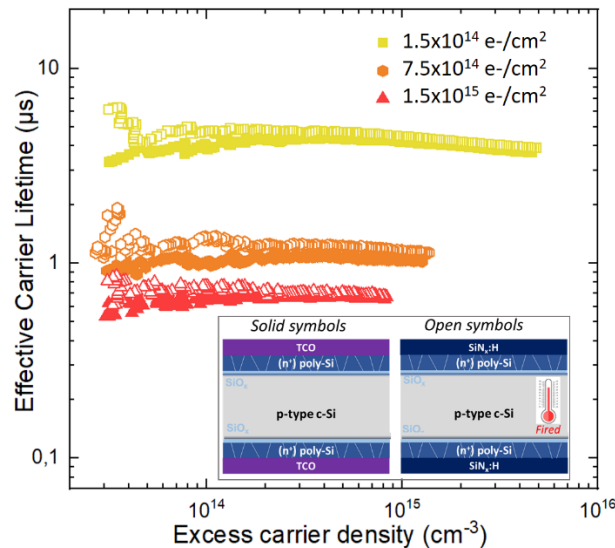


Figure 3. Effective carrier lifetime as a function of the excess carrier density, for different irradiation fluences (20 $\Omega\cdot\text{cm}$ Ga-doped sample).

Subsequently, the 20 $\Omega\cdot\text{cm}$ Ga-doped samples which experienced the hydrogenation step were placed on a hot plate under prolonged illumination (halogen lamp, $0.1 \text{ W}\cdot\text{cm}^{-2}$). They experienced first 500 hours of prolonged illumination at 80°C. Then, the temperature was increased to 100°C. At different time intervals, the samples were removed from the hot plate and τ_{eff} measurements were conducted at room temperature. Fig. 4 presents the τ_{eff} evolution. It is

worth noticing that the τ_{eff} values are perfectly stable over the studied period of time, even after having increased the temperature from 80°C to 100°C. Compare to the samples studied in [3], which feature strong recovery effects under illumination, the fact that our samples are not subjected to such mechanisms could first originate from a lack of H in the bulk (large amounts of H could be for instance trapped in the vicinity of the ultra-thin SiO_x layer, as shown in [9]). This could also be due to the fact that the bulk hydrogenation should be combined with complementary levers (such as lower substrate thicknesses, as indicated in [3]) in order to observe efficient recovery mechanisms.

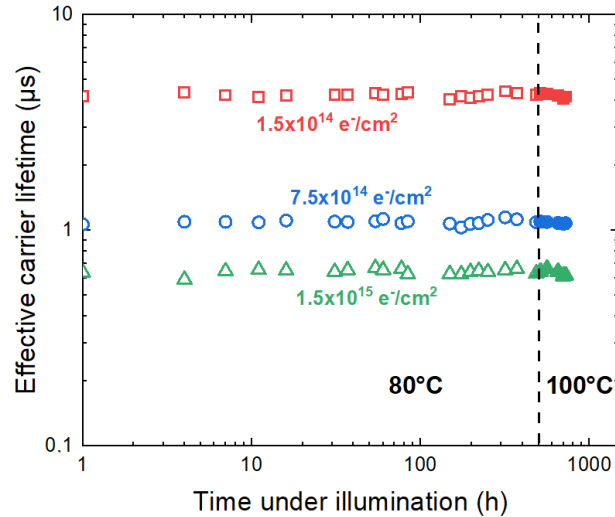


Figure 4. Evolution of the effective carrier lifetime under illumination (20 Ω .cm Ga-doped sample). Effective lifetime values were extracted for an excess carrier density of $1 \times 10^{14} \text{ cm}^{-3}$.

4. Conclusions

This study successfully demonstrated that solar cells with poly-Si-based passivated contacts (i.e., TOPCon) could be adapted to the main prerequisites for space missions. Indeed, flexible and lightweight alternative TOPCon cells were prepared from gallium-doped substrates, with post-irradiation performances as good as those of conventional (3 times thicker, 60 μm vs. 180 μm) PERC devices. The influence of the doping level was investigated. Low doping levels mitigate the radiation-induced degradation of τ_b and therefore of the J_{sc} , but result in lower V_{oc} . Furthermore, it was shown that the surface and bulk hydrogenation step investigated throughout this study does not influence the post-irradiation τ_{eff} and its evolution under prolonged illumination in the temperature range 80°C-100°C (at least for the durations investigated here).

Data availability statement

The data collected supporting the findings are available from the corresponding author upon reasonable request.

Author contributions

N. Enjalbert: project administration, conceptualization, methodology, formal analysis, investigation, writing – review & editing; **R. Cariou:** funding acquisition, conceptualization, formal analysis, investigation, writing – review & editing; **S. Dubois:** funding acquisition, resources, methodology, formal analysis, writing – review & editing.

Competing interests

The authors declare that they have no competing interests.

Funding

This research was supported by ESA via a Discovery element contract N° 4000138622. This work reflects only authors view and not the one of ESA. ESA is not responsible for any use that may be made of the information it contains.

References

1. M. Yamagushi *et al.*, "Analysis for nonradiative recombination loss and radiation degradation of Si space solar cells", Prog. in Photovoltaics: Research and Applications, vol. 29, no.1, pp. 98-108, Sept., 2021, doi: <https://doi.org/10.1002/pip.3346>
2. V. Mihailetchi *et al.*, "Suitable Si solar cell technologies for use in space applications", Proceedings of the 38th European Photovoltaic Solar Energy Conference and Exhibition, pp. 1092-1095, 2021, doi: <https://doi.org/10.4229/EUPVSEC20212021-5EO.2.1>
3. A. Fedoseyev *et al.*, "Radiation effects model for Ultra-Thin Silicon Solar Cells", Journal of Physics: Conference Series, vol. 2675, no. 1, pp. 012012, Dec., 2023, doi: <https://doi.org/10.1088/1742-6596/2675/1/012012>
4. M. U. Khan *et al.*, "Degradation and regeneration of radiation-induced defects in Si: a study of vacancy-hydrogen interactions", Sol. Ener. Mat. & Sol. Cells, vol. 200, pp. 109990, Sept., 2019, doi: <https://doi.org/10.1016/j.solmat.2019.109990>
5. R. Cariou *et al.*, "Investigation of p-type Silicon Heterojunction Radiation Hardness", IEEE Journal of Photovoltaics, vol. 14, no. 1, Nov., 2023, <https://doi.org/10.1109/JPHOTOV.2023.3333197>
6. T. Desrues *et al.*, "Poly-Si/SiO_x Passivating Contacts on Both Sides: A Versatile Technology For High Efficiency Solar Cells", proceedings of the IEEE 48th Photovoltaic Specialists Conference (PVSC), pp. 1069-1072, 2021, <https://doi.org/10.1109/PVSC43889.2021.9518773>
7. V. Bocquet *et al.*, "Tracking Hydrogen During Poly-Si/SiO_x Contact Fabrication: An Infrared Spectroscopy Analysis of Si-H Bonds Configurations", SiliconPV Conference Proceedings, Feb., 2024, <https://doi.org/10.52825/siliconpv.v1i.847>
8. A. Khan *et al.*, "Role of the impurities in production rates of radiation-induced defects in silicon materials and solar cells", Journal of Applied Physics, vol. 90, no. 3, pp. 1170-1178, 2001, <https://doi.org/10.1063/1.1384855>
9. A. Morisset *et al.*, "Evolution of the surface passivation mechanism during the fabrication of ex-situ doped poly-Si(B)/SiO_x passivating contacts for high efficiency c-Si solar cells", Sol. Energy Mater. Sol. Cells, vol. 221, pp. 110899, March, 2021, <https://doi.org/10.1016/j.solmat.2020.110899>